Xiong Z, Ren S, Chen H, Liu Y, Huang C, Zhang YL, Odera JO, Chen T, Kist R, Peters H, Garman K, Sun Z, Chen X.

PAX9 regulates squamous cell differentiation and carcinogenesis in the oro-esophageal epithelium.

***Journal of Pathology* 2017**

DOI: https://doi.org/10.1002/path.4998

PAX9 regulates squamous cell differentiation and carcinogenesis in the oro-esophageal epithelium

Zhaohui Xiong[a,b,1], Shuang Ren[a,b,1], Hao Chen[b], Yao Liu[a,b], Caizhi Huang[b], Yawan Lyvia Zhang[b], Joab Otieno Odera[b], Tong Chen[c], Ralf Kist[d,e], Heiko Peters[e], Katherine Garman[f], Zheng Sun[a,*] and Xiaoxin Chen[b,g,*]

[a] Department of Oral Medicine, Beijing Hospital for Stomatology, Capital Medical University, 4 Tian-Tan-Xi-Li, Beijing 100050, China

[b] Cancer Research Program, Julius L. Chambers Biomedical Biotechnology Research Institute, North Carolina Central University, 700 George Street, Durham, NC 27707, USA

[c] Division of Medical Oncology, Department of Internal Medicine, The Ohio State University, 410 West 12 Avenue, Columbus, OH 43210, USA

[d] Centre for Oral Health Research, School of Dental Sciences, Newcastle University, Framlington Place, Newcastle upon Tyne, NE2 4BW, UK

[e] Institute of Human Genetics, Newcastle University, International Centre for Life, Central Parkway, Newcastle upon Tyne, NE1 3BZ, UK

[f] Division of Gastroenterology, Department of Medicine, Duke University, DUMC 3913, Durham, NC 27710, USA

[g] Center for Gastrointestinal Biology and Disease, Division of Gastroenterology and Hepatology, Department of Medicine, University of North Carolina at Chapel Hill, Chapel Hill, NC 27599,

This article has been accepted for publication and undergone full peer review but has not been through the copyediting, typesetting, pagination and proofreading process, which may lead to differences between this version and the Version of Record. Please cite this article as doi: 10.1002/path.4998

USA

[1] These authors contributed equally to this work.

*** Co-corresponding authors:** Zheng Sun, D.D.S, PhD, Beijing Stomatological Hospital & School of Stomatology, Capital Medical University, 4 Tiantanxili, Dongcheng District, Beijing 100050, China. Tel: 86-10-67099016; Fax: 86-10-67013995; Email: sunzheng12@vip.126.com; Xiaoxin Luke Chen, MD, PhD, Cancer Research Program, Julius L. Chambers Biomedical Biotechnology Research Institute, North Carolina Central University, 700 George Street, Durham, NC 27707, USA. Tel: 919-530-6425; Fax: 919-530-7780; Email: lchen@nccu.edu

Running title: PAX9 and oro-esophageal squamous cell carcinoma

Conflict of interest: The authors declare no potential conflicts of interest.

Abbreviations: DAC, 5-aza-2′-deoxycytidine; ESCC, esophageal squamous cell carcinoma; OESCC, Oro-esophageal squamous cell carcinoma; OR, odds ratio; SAM, significance analysis of microarrays;

Abstract

PAX9 is a transcription factor of the PAX family characterized by a DNA-binding paired domain. Previous studies have suggested a potential role of PAX9 in squamous cell differentiation and carcinogenesis of the oro-esophageal epithelium. However, its functional roles in differentiation and carcinogenesis remain unclear. In this study, *Pax9* deficiency in the mouse esophagus promoted cell proliferation, delayed cell differentiation and altered the global gene expression profile. Ethanol exposure down-regulated PAX9 expression in human esophageal epithelial cells *in vitro* and mouse forestomach and tongue *in vivo*. We further

showed that PAX9 was down-regulated in human oro-esophageal squamous cell carcinoma (OESCC), and its down-regulation was associated with alcohol drinking and promoter hypermethylation. Moreover, *ad libitum* feeding with a liquid diet containing ethanol for 40 weeks or *Pax9* deficiency promoted *N*-nitrosomethylbenzylamine-induced squamous cell carcinogenesis in mouse tongue, esophagus, and forestomach. In conclusion, PAX9 regulates squamous cell differentiation in the oro-esophageal epithelium. Alcohol drinking and promoter hypermethylation are associated with PAX9 silencing in human OESCC. PAX9 down-regulation may contribute to alcohol-associated oro-esophageal squamous cell carcinogenesis.

Keywords: PAX9; Esophagus; Ethanol; Promoter hypermethylation; Squamous cell carcinoma.

Introduction

PAX9 is a transcription factor of the PAX family characterized by a DNA-binding paired domain. Being expressed in somites, pharyngeal pouches, and mesenchyme, PAX9 is essential for the development of thymus, parathyroid, limb, palate, and teeth during mouse embryogenesis. Homozygous *Pax9* knockout mice die shortly after birth due to cleft palate [1]. Subsequent studies have also clearly demonstrated an essential role of PAX9 in the development of filiform papilla and taste bud of the tongue, lip, and intervertebral disc [2-5]. However, in adults, PAX9 expression is restricted to the endocrine tissues (e.g., thymus, parathyroid) and the upper gastrointestinal tract (e.g., tongue, esophagus, salivary gland, cheek epithelium), with the strongest expression in the tongue [6].

Previous studies have suggested a potential role for the absence of PAX9 in human esophageal squamous cell carcinoma (ESCC) and oral squamous cell carcinoma (OSCC). In human ESCC tissue samples, PAX9 was found to be lost or down-regulated, and progressive loss of PAX9 expression was correlated with increasing malignancy [7]. PAX9 expression was associated with better survival and radiosensitivity [8]. In human OSCC cells, PAX9 expression was essential for cell growth and survival [9]. In Barrett's esophagus, a human disease characterized by intestinal metaplasia of esophageal squamous epithelium, PAX9 was found to be down-regulated [10], suggesting its involvement in squamous differentiation. *Pax9* and its downstream genes were involved in the terminal maturation of esophageal epithelium of mouse esophagus [11]. Moreover, morpholino-knockdown of *pax9* in zebrafish resulted in loss or disorganization of the squamous epithelium in the tongue [12]. These evidence support the hypothesis that PAX9 may regulate squamous epithelial cell differentiation in the adult oro-esophageal epithelium.

In this study, we aimed to understand the functional role of PAX9 in the oro-esophageal epithelium using tissue-specific PAX9-deficient mice, human cells and tissues.

Materials and Methods

Human tissue samples

Human ESCC and OSCC tissue samples were obtained from Duke University Medical Center and Beijing Stomatological Hospital, respectively, with informed written consent and institutional IRB approval (Pro39682 and Pro56638). All human samples (n=26) were coded with patient identifiers removed. Clinical data including alcohol exposure were collected from the medical record. Patients with a self-reported history of alcohol drinking (n=15) were regarded as "drinker" (5 drinks/week on average), and those who reported never drinking alcohol (n=5) as "non-drinkers". Occasional drinkers (n=6) were excluded from further analysis on the association between alcohol drinking and PAX9 expression. A human ESCC tissue array with tumors and matched normal adjacent tissues (Cat #: HEso-Squ060PG-01) and a human OSCC array with tumors and non-matched normal tissues (Cat #: OR601b) were purchased from US Biomax (Derwood, MD, USA).

Cell culture and treatments

Human ESCC cells, KYSE510, KYSE450, and KYSE70, were obtained from ATCC (Manassas, VA, USA) and ECACC (Porton Down, Salisbury, UK) with proper authentication. KYSE510 and KYSE450 cells were exposed to ethanol. KYSE70 cells were treated with 5-aza-2'-deoxycytidine (DAC; Sigma-Aldrich, St. Louis, MO, USA) for 72 h.

Animal experiments

All animal experiments were approved by the IACUC at the North Carolina Central University. *Krt5*Cre mice [13] and *Pax9*$^{loxP/loxP}$ mice [14] were crossed to generate tissue-specific *Pax9*-deficient mice (*Krt5*Cre;*Pax9*$^{loxP/loxP}$). Tissue samples (tongue, esophagus, forestomach) were harvested for analysis of morphology, gene expression and transmission electron

microscopy (TEM).

In an ethanol exposure study, wild-type C57BL/6J mice (Jackson Laboratory, Bar Harbor, ME) were given *ad libitum* water, or 20% ethanol (plus 0.3% saccharin) in the drink for 4 weeks, or 15% alcohol (plus 0.3% saccharin) in the drink for 40 weeks.

In a carcinogenesis study, *N*-nitrosomethylbenzylamine (NMBA) was used to induce tumorigenesis in mouse esophagus and forestomach [15]. Mice were given six intragastric doses of NMBA (Ash Stevens, Riverview, MI, USA) at 2 mg/kg body weight twice each week for 3 weeks. Wild-type C57BL/6J mice were given *ad libitum* the *Lieber-DeCarli* Regular Control diet (710027; Dyets Inc., Bethlehem, PA, USA) (Group A), or an isocaloric *Lieber-DeCarli* diet plus 6.4% v/v ethanol (710260; Dyets) (Group B). *Lieber-DeCarli* diet is a high-fat, nutritionally complete liquid diet, which was designed to partially overcome the murine dislike of ethanol [16]. *Pax9*-deficient mice were given the control liquid diet (Group C) (Table 1). All mice were sacrificed at 40 weeks and analyzed for tumorigenesis in tongue, esophagus, and forestomach. The number of macroscopically visible tumors (≥0.5 mm in diameter) in mouse forestomach and tongue was scored. Tissues were processed routinely for paraffin sectioning (5 μm), H&E staining and histopathology. Microscopic lesions including dysplasia, papilloma, and SCC were diagnosed according to established criteria [15].

Western blotting

Protein was isolated from the human ESCC cells and mouse tissues using a standard method. In brief, tissue lysates were prepared by homogenizing tissue with the TissueLyser bead mill (Qiagen, Valencia, CA, USA) in RIPA buffer (Sigma-Aldrich). Cell debris was removed by a short centrifugation and an aliquot of cleared lysate was kept for protein quantitation using the BCA Protein Assay Kit (Biorad, Hercules, CA, USA). Proteins were detected with a rabbit

monoclonal anti-PAX9 (1:600, Cat #: 12847, Cell Signaling Technology, Danvers, MA, USA) and a mouse monoclonal anti-GAPDH antibody (1:50000, ab8245, Abcam, Cambridge, MA, USA).

Histochemical staining, immunohistochemical staining (IHC), TUNEL assay and immunofluorescent staining

Haematoxylin & eosin staining was conducted based on a routine protocol. For IHC staining, deparaffinized sections were pre-treated to retrieve antigens using a Tris-based Antigen Unmasking Solution (Vector Laboratories, Burlingame, CA, USA), prior to incubation with either a rabbit monoclonal anti-PAX9 (1:400, Cell Signaling Technology), a rat monoclonal anti-BrdU (1:1000, ab6326, Abcam), a rabbit polyclonal anti-loricrin (1:500, ab24722, Abcam), a mouse monoclonal anti-proliferating cell nuclear antigen (PCNA; 1:3000, P8825, Sigma-Aldrich), a rabbit monoclonal anti-SOX2 (1:100, ab92494, Abcam), a rabbit polyclonal anti-FOXA3 (1:100, PA1-17038, Affinity Bioreagents, Golden, CO, USA), a rabbit polyclonal anti-WNT3 (1:100, ab32249, Abcam), a rabbit polyclonal anti-SFRP5 (1:50, LS-C169017, LifeSpan Biosciences, Seattle, WA), a guinea pig polyclonal anti-KRT35 (1:200, LS-C20268, LifeSpan Biosciences), a rabbit monoclonal anti-KRT5 (1:200, RM-2106-S0, Thermo Scientific, Rockford, IL), a rabbit polyclonal anti-P63 (1:100, GTX102425, GeneTex, Irvine, CA, USA), a rabbit polyclonal anti-involucrin (1:500, 924401, BioLegend, San Diego, CA, USA) or a rabbit polyclonal anti-filaggrin (1:100, GTX37695, GeneTex) overnight at 4 °C. The percentage of positively stained epithelial cells was calculated. Three sections were counted for each sample.

A terminal deoxynucleotidyl transferase dUTP nick end labeling (TUNEL) assay was conducted according to the protocol provided by the manufacturer of the TACS^{TM} TDT kit (R&D Systems, Minneapolis, MN, USA). The apoptotic index was calculated by dividing the number

of TUNEL positive cells by the total number of epithelial cells.

We performed immunofluorescent double staining for BrdU and Ki67 to test whether the BrdU-positive cells that were retained in the epithelial layer were still proliferating 5 days after pulse-labeling (50 mg/kg, *i.p.*) [17]. Immunofluorescent double staining was conducted based on standard procedures. Ki67 and BrdU were detected by a rabbit anti-Ki67 (1:200, RM-9106, Thermo Scientific) and a rat monoclonal anti-BrdU (1:1000, ab6326, Abcam) overnight at 4 °C, and then by a goat-anti-rabbit Alexa 568 and goat-anti-rat Alexa 488 (1:1000, A-11008 and A-11077, Thermo Scientific).

Transmission electron microscopy (TEM)

Mouse tissue was fixed with 4% glutaraldehyde in cacodylate buffer for at least one hour. Thick and thin sections were prepared on a Reichert-Jung ultramicrotome (Leica, Bannockburn, IL). Thick sections were stained with 1% toluidine blue-borax for selection using light microscopy of the appropriate areas for thin sections. Thin sections were prepared, mounted on copper grids, and double stained for examination using a Philips CM 12 electron microscope (FEI, Hillsboro, OR).

Gene microarray analysis

For gene microarray analysis, total RNA was extracted from mouse forestomach, or mouse esophageal epithelium with an RNeasy Fibrous Tissue Mini Kit (Qiagen), according to the manufacturer's instructions. Microarray experiments were performed with Agilent mouse 4x44k microarrays. The raw data has been submitted to NCBI's GEO database (series GSE75373, GSE96735). As previously described [11], differentially expressed genes were obtained from two-class significance analysis of microarrays (SAM) in Excel with the median number of false positives less than 1. Gene set analysis (GSA) was carried out as an add-in in Excel with

curated gene sets in three major categories: Canonical Pathway (CP), Gene Ontology (GO) and Transcription Factor (TF). Knowledge-based gene sets (KB) were generated based on the literature and have been successfully used in our previous microarray study [11]. The *Pax9* gene set was based on a list of genes differentially expressed in *Pax9* knockout mice [2]. Hierarchical clustering analysis and principal component analysis (PCA) were performed using the R package. Microarray data of four GEO datasets (GSE23400, GSE20347, GSE13601, GSE6631) were downloaded and analyzed to compare *PAX9* mRNA expression in cancer versus matched normal tissue.

Pyrosequencing of the human *PAX9* gene promoter and mouse *Pax9* gene promoter

Genomic DNA was purified using a DNeasy Tissue kit (Qiagen) according to the manufacturer's instructions. DNA methylation level in the *PAX9* gene promoter region was determined by EpigenDx Inc (Worcester, MA, USA) using the PSQ™96 HS system (Qiagen) according to standard procedures with a unique set of primers. The methylation status of each CpG site in the promoter regions (supplementary material, Figure S7) was determined individually as an artificial C/T SNP using QCpG software (Qiagen). A series of unmethylated and methylated DNA were included as controls in each PCR.

RT-PCR, qRT-PCR and chromatin immunoprecipitation (ChIP)

For regular RT-PCR, total RNA was reverse transcribed using the Advantage RT-for-PCR kit (Clontech), according to the manufacturer's instructions. *Pax9* exon 2 was detected with the following primer pairs (predicted size: 278 bp): *Pax*9F (5'-ACCACATTTACTCATATCCCAGTCCCA-3') and *Pax*9R (5'–GGCTCCCTTCTCCAATCCATTCA-3').

Quantitative PCR was performed on cDNA pools to assess the expression levels of genes of interest with primers and probes obtained from Applied Biosystems Inc. (Foster City, CA) using TaqMan and 96-well optical plate using A ABI 7900HT Fast Real-Time PCR system in triplicate.

PAX9 binding sites within the 5'-upstream DNA sequence of *Krt35* (ENSMUSG00000048013) were predicted using Anchored Combination TFBS Cluster Analysis (oPOSSUM version 3.0). ChIP analysis was performed in triplicate using an EZ-ChIP kit (Millipore, Billerica, MA, USA) according to the manufacturer's instructions with the above-mentioned anti-PAX9. Immunoprecipitated DNA or input was PCR amplified with the following primer pairs: *Krt35* (5'-CCACATCCTGAGTTCAATCC-3' and 5'-CCAAGACAGGATCTCTCATTAC-3'; predicted size=174 bp); negative control *P63* (5'-CAAATGTTGCTTGTCTGGTG-3' and 5'-GTCAGTCGAGTGCACAGTTT-3'; predicted size=210 bp).

Statistical analyses

GraphPad Prism 6 (GraphPad Software, La Jolla, CA, USA) was used for Student's t-test, Fisher's exact test and McNemar's test, with the statistical significance level set at 0.05. All comparisons were two-sided.

Results

Esophageal phenotypes of *Krt5*Cre;*Pax9*$^{loxP/loxP}$ mice

To elucidate the function of PAX9 in the oro-esophageal epithelium *in vivo*, *Pax9* was inactivated in stratified squamous epithelial cells by crossing *Krt5*Cre mice and *Pax9*$^{loxP/loxP}$ mice resulting in *Krt5*Cre;*Pax9*$^{loxP/loxP}$ mice. Whereas *Pax9* knockout mice die after birth [1], *Krt5*Cre;*Pax9*$^{loxP/loxP}$ mice appeared healthy and bred normally. *Pax9* deficiency in the esophagus was validated by RT-qPCR (supplementary material, Figure S1A) and IHC (supplementary material, Figure S1B-E). IHC for PCNA showed epithelial hyperproliferation in *Pax9*-deficient esophagus (supplementary material, Figure S1F-H).

Papilloma-like structures were formed in the squamous epithelium of *Pax9*-deficient esophagus (Figure 1B, D) as compared with control esophagus (Figure 1A, C). Hyperproliferation was evident with an increased number of BrdU-positive cells (Figure 1E-H). Apoptosis as detected by a TUNEL assay was slightly different between *Pax9*-deficient esophagus (0.7±0.4%, Figure 1J) and control esophagus (0.2±0.1%, Figure 1I). Toluidine blue staining showed increased keratohyalin granules in the keratinized cells and palisading of basal cells in the mutant esophagus (Figure 1K, L). Under TEM, in the basal layer of mutant esophagus, the intercellular space, desmosomes and adhesion fingers between cells were disorganized (Figure 1M, N). At the fifth day following a BrdU pulse injection, some suprabasal cells of mutant esophagus remained strongly positive for BrdU and Ki67 (Figure 1P, R, T, V; yellow arrows) as compared with the control esophagus (Figure 1O, Q, S, U), suggesting that migration of these cells toward the lumen was impaired.

Gene microarray analysis showed that 60 genes were down-regulated of which some were associated with squamous cell differentiation (e.g., *Krtap3-3*, *Krt1-24/Krt35*, *Sfrp5*), and 83

genes were up-regulated in *Pax9*-deficient mice (e.g., *Wnt3*, *Foxa3, Gata3*) (Figure 2A). Multiple gene sets were enriched in control esophagus including "*Pax9* target genes". Several gene sets were enriched in the *Pax9*-deficient esophagus, e.g., "basal layer", "*Sox2* target genes", "cell-cell junction" (supplementary material, Table S1). RT-qPCR showed up-regulation of hedgehog pathway genes (*Gli1*, *Gli2*), Wnt pathway genes (*Wnt3*, *Gata3*), and genes highly expressed in basal cells (*Sox2*, *P63*), and down-regulation of *Pax9* and its downstream genes (*Krt35*) (supplementary material, Figure S2A). ChIP-PCR confirmed PAX9 binding to the 5' upstream DNA sequence of *Krt35* gene (supplementary material, Figure S2B). IHC for the selected genes involved in epithelial differentiation showed up-regulation of SOX2 (Figure 2B, C), FOXA3 (Figure 2D, E), WNT3 (Figure 2F, G) and KRT5 (Figure 2L, M), slightly increase of P63 expression (Figure 2N, O), and down-regulation of SFRP5 (Figure 2H, I), KRT35 (Figure 2J, K) and loricrin (Figure 2T, U) in the esophageal epithelium of *Pax9*-deficient mice. An obvious change in expression of filaggrin (Figure 2P, Q) or involucrin (Figure 2R, S) was not observed.

PAX9 is down-regulated in human ESCC and OSCC

To examine the clinical relevance of PAX9 down-regulation, we analyzed microarray data of four GEO datasets (GSE23400, GSE20347, GSE13601, and GSE6631) and these showed significant down-regulation of *PAX9* mRNA in human ESCC (supplementary material, Figure S3A, B) and human OSCC (supplementary material, Figure S3C, D), as compared with matched normal tissues.

Using two commercially available tissue microarrays, we obtained positive PAX9 staining in 2/29 ESCC and 25/29 matched normal esophagus ($p<0.0001$), and in 6/50 OSCC and 6/10 normal oral mucosa ($p=0.0026$).

Using our human samples, IHC showed a dramatic decrease of PAX9 expression in ESCC

versus adjacent normal esophageal tissues (Figure 3C, D, E). ESCC and adjacent normal esophageal tissue were confirmed by H&E staining (Figure 3A, B). Interestingly, based on the alcohol-drinking status of these patients (drinker or non-drinker), a significant decrease of PAX9-positive cells was observed in drinker's normal tissue as compared to normal tissue from the non-drinkers (Figure 3F). Even in cancer tissues, a slight decrease of PAX9 expression was also observed in drinker's when compared to non-drinker's tissue.

Ethanol down-regulates PAX9 expression in oro-esophageal squamous epithelial cells *in vitro* and *in vivo*

Time- and dose-dependent exposure of KYSE510 and KYSE450 cells to ethanol confirmed down-regulation of PAX9 expression as shown by Western blotting (supplementary material, Figure S4). To further understand the effects of ethanol on PAX9 and global gene expression *in vivo*, mice were exposed to 20% sweetened ethanol for 4 weeks, or 15% sweetened ethanol for 40 weeks. H&E staining showed the thickness of the epithelium increased (Figure 4A, B, C) in those exposed to 15% ethanol for 40 weeks. Proliferation increased in response to ethanol at both 4 weeks (20% alcohol) and 40 weeks (15% alcohol): IHC for BrdU showed a significant increase of BrdU-positive epithelial cells in mouse forestomach (Figure 4D, E, F, G), indicating increased cell proliferation as a result of ethanol exposure *in vivo*.

Thirty-two genes were down-regulated by 20% ethanol for 4 weeks, and 581 genes up-regulated and 1,506 genes down-regulated by 15% ethanol for 40 weeks, as compared with control (supplementary material, Table S2). Using GSA analysis, we found enrichment of multiple gene sets including "*Pax9* target genes" and "epidermal differentiation complex" in control forestomach, suggesting downregulation of *Pax9* target genes by ethanol exposure (Figure 4H). PCA analysis and clustering analysis also supported distinct gene expression

profiles of three groups (supplementary material, Figure S5).

IHC staining showed reduced expression of loricrin (a marker of squamous cell differentiation) in ethanol-exposed forestomach as compared with control (Figure 4I, J, K), indicating that squamous differentiation was suppressed by ethanol. Down-regulation of PAX9 expression in mouse forestomach was also observed (Figure 4L, M, N), especially in those exposed to 15% ethanol for 40 weeks. *Pax9* down-regulation was further confirmed by Western blotting and RT-qPCR (Figure 4O, P, Q). In addition to the forestomach, ethanol-exposed mouse tongue also expressed PAX9 at a reduced level as shown by Western blotting and IHC (Supplementary material, Figure S6). No obvious change of PAX9 expression was observed in mouse esophagus (data not shown).

Promoter hypermethylation is associated with *PAX9* silencing in human ESCC cells and OSCC tissues

To understand the molecular mechanism through which alcohol drinking down-regulates PAX9 expression, CpG sites in the promoter regions of two different *PAX9* transcriptional start sites (supplementary material, Figure S7) were pyrosequenced in control and DAC-treated KYSE70 cells. Consistent with an increase in PAX9 expression (Figure 5A), the methylation level of DAC-treated KYSE70 cells was lower than that of control (Figure 5B). More importantly, the methylation levels of both transcripts were higher in OSCC tissue samples than in matched normal samples (Figure 5C).

We then pyrosequenced the promoter regions of two different *PAX9* transcriptional start sites in ethanol-exposed KYSE510 cells (100 mM for 72 h) and mouse forestomach (15% for 40 weeks). Despite the decrease in PAX9 expression, no significant difference of methylation levels was found between control samples and ethanol-exposed samples (supplementary material,

Figure S8).

Increased susceptibility to NMBA-induced oro-esophageal squamous cell carcinogenesis in *Krt5*Cre;*Pax9*$^{loxP/loxP}$ mice

To determine whether *Pax9* deficiency promotes OESCC, wild-type or *Pax9*-deficient mice were given six intragastric doses of NMBA and sacrificed at 40 weeks. The number of macroscopically visible tumors in mouse forestomach was significantly increased in *Pax9*-deficient mice, as compared with control (Figure 6A). Seven *Pax9*-deficient mice developed tongue tumors. Similar to *Pax9* deficiency, an isocaloric *Lieber-DeCarli* diet containing ethanol for 40 weeks also significantly enhanced forestomach tumorigenesis in wild-type mice as compared with a control liquid diet.

Under the microscope, the incidence of esophageal papilloma was significantly increased in ethanol-exposed mice, as compared with control. Incidences of forestomach dysplasia and SCC significantly increased from 22.2% and 5.6% in control mice to 81.8% and 31.8% in *Pax9*-deficient mice. The incidence of tongue lesions (dysplasia, papilloma, and SCC) was also significantly increased from 0% in control mice to 36.4% in *Pax9*-deficient mice (Table 1) (Figure 6B-I). IHC showed that PAX9 expression was not dramatically altered in histologically normal epithelium of NMBA-treated mice (supplementary material, Figure S9A, B). However, PAX9 expression was down-regulated during forestomach carcinogenesis as shown by decreasing expression from histologically normal to dysplasia and cancer (supplementary material, Figure S9B-D)

Discussion

This study is the first to demonstrate functional roles of PAX9 in the adult oro-esophageal epithelium. Tissue-specific *Pax9* deficiency was associated with squamous epithelial cell hyperproliferation, delayed cell differentiation and altered global gene expression profile in mouse esophagus. PAX9 down-regulation was confirmed in human OESCC and associated with alcohol drinking. Ethanol exposure down-regulated PAX9 expression in oro-esophageal squamous epithelial cells *in vitro* and *in vivo*. Promoter hypermethylation was found to be associated with *PAX9* silencing in human OESCC. Furthermore, both *Pax9* deficiency and ethanol exposure promoted OESCC *in vivo*.

As a transcription factor, PAX9 is expressed in adult squamous epithelial cells in the upper gastrointestinal tract with the strongest expression in the tongue [6]. Clinically, *PAX9* mutations have been reported in patients with oligodontia and cleft palate [18,19]. Previous studies by us and others have suggested a potential role of PAX9 in squamous cell differentiation and carcinogenesis [7,9-12]. In this study, *Pax9* deficiency enhanced epithelial cell proliferation (papilloma-like structure, an increase of BrdU-labeling index and PCNA expression) and inhibited cell differentiation (loricrin downregulation, delayed maturation of BrdU-labelled cells) in mouse esophagus (Figure 1, 2).

Using GEO datasets and our own tissue samples, we further confirmed PAX9 down-regulation in human ESCC and OSCC (supplementary material, Figure S3 and Figure 3). Although human ESCC with a low level of PAX9 expression does share similarities in gene expression with Pax9-deficient esophagus (data not shown), it should be noted that mouse array and human array did not test the same genes, particularly in the early days. Therefore, such a relevance should be treated with caution. An interesting association between PAX9

down-regulation and alcohol drinking in human ESCC led us to investigate whether alcohol drinking, a major risk factor for OESCC [20-22], may cause PAX9 down-regulation. In fact, OSCC has a stronger association with alcohol exposure than cancers of any other organ sites [23-25]. A case-control study on the risk of ESCC showed a higher odds ratio (OR) for heavy drinkers (OR=10) compared to tobacco smokers (OR=5.8). Heavy drinking led to an increased numbers of SCC and dysplastic lesions in the human esophagus [26,27]. Acetaldehyde, an ethanol metabolite, is believed to be a carcinogen that contributes to the development of ESCC. Genetic polymorphisms of ethanol-metabolizing genes, such as acetaldehyde dehydrogenase and alcohol dehydrogenase, are also strongly and consistently associated with OESCC [21,22]. Our data showed that ethanol exposure caused time- and dose-dependent decrease of PAX9 expression in esophageal epithelial cells *in vitro* (supplementary material, Figure S4). More importantly, ethanol exposure reduced PAX9 expression in mouse forestomach (Figure 4) and tongue (supplementary material, Figure S6). It was unexpected that PAX9 expression in mouse esophagus was not significantly affected by ethanol exposure. Presumably, short duration of contact may account for relatively weak effect of ethanol on the esophageal epithelium.

We next aimed to understand the molecular mechanism leading to *PAX9* silencing in OESCC. *PAX9* has been identified as a gene subject to promoter methylation in human ESCC and in lung cancer [28,29]. A genome-wide DNA methylome analysis revealed widespread ethanol-induced alterations with significant hypermethylation of many regions of chromosomes in human embryonic stem cells [30]. We, therefore, pyrosequenced the promoter regions of two different *PAX9* transcriptional start sites (supplementary material, Figure S7). Consistent with our hypothesis, the methylation percentages of multiple CpG sites in OSCC samples were significantly higher than those of matched normal tissues (Figure 5C). A demethylating agent

increased PAX9 expression in KYSE70 cells and meanwhile reduced CpG methylation percentages (Figure 5A, B). However, ethanol exposure of KYSE510 cells or mouse forestomach did not result in *PAX9* promoter hypermethylation even though PAX9 expression was down-regulated (supplementary material, Figure S8). Our data suggested alternative mechanisms are responsible for PAX9 down-regulation by ethanol in our experimental settings. However, we cannot exclude the possibility that our experimental settings, *i.e.*, ethanol exposure of cells and feeding mice with ethanol, may not exactly reproduce sequential changes leading to *PAX9* silencing in human OESCC. It remains unknown whether promoter hypermethylation may be associated with PAX9 down-regulation due to alcohol drinking.

Our last question was whether *Pax9* deficiency contributes to OESCC *in vivo*. In *Pax9*-deficient mice, we observed a significant increase in the number of forestomach tumors and the incidences of esophageal and forestomach lesions (papilloma, dysplasia, SCC) (Table 1, Figure 6). Because NMBA is not expected to induce tumors in the tongue of wild-type mice [15], development of tongue lesions in *Pax9*-deficient mice further supported the importance of PAX9 down-regulation in the development of OESCC. Consistent with the association between alcohol drinking and PAX9 down-regulation, feeding mice with an isocaloric liquid diet containing ethanol significantly increased the number of forestomach papilloma and the incidence of esophageal papilloma (Figure 6A, Table 1). Based on the gene expression data, we speculate that PAX9 down-regulation may allow activation of multiple oncogenic pathways, and thus facilitates OESCC. For example, Shh signaling activation results in the expansion of epithelial precursor cell compartment [17]. Of note, hedgehog ligand is required for the growth of digestive tract tumors including esophageal cancer [31]. Wnt signaling is involved in early differentiation of esophageal epithelium [11]. In OESCC, poor histological differentiation and clinical outcome are

associated with increased expression of nuclear β-catenin [32]. Exposure to carcinogen and ethanol increases overall β-catenin level in the tongue [33]. *Sox2* and *P63* colocalized at genetic loci and co-regulated gene expression to facilitate the development of ESCC [34]. Transgenic overexpression of SOX2 itself was found to induced SCC in mouse forestomach [35] and lung [36]. It should be noted that humans do not have forestomach. Therefore enhanced forestomach carcinogenesis by *Pax9* deficiency may or may not be relevant to human ESCC.

Taken together, PAX9 regulates squamous cell differentiation and carcinogenesis in the oro-esophageal epithelium. Our data support a novel mechanism that PAX9 down-regulation may also contribute to alcohol-associated OESCC. Further studies are warranted to understand upstream events leading to PAX9 down-regulation by ethanol, and downstream mechanisms which promote OESCC.

Acknowledgments: The authors acknowledge excellent microarray service by Dr. Yan Shi and her staff at the Genomics Core Facility, Lineberger Comprehensive Cancer Center, University of North Carolina at Chapel Hill, Chapel Hill, NC. The authors also thank Dr. Sara E. Miller and Mr. Phillip Christopher at the Department of Pathology, Duke University, Durham, NC, for their excellent electron microscopy service. The pyroseqencing service provided by Dr. Liying Yan at EpigenDx Inc. is greatly appreciated. This work was supported by research grants from the National Natural Science Foundation of China (grant numbers 30973325, 81372897) and the National Institutes of Health (grant numbers U54 AA019765, U54 CA156735).

Author Contributions: ZX, SR, HC, YL, CH, LZ, and JO conducted the experiments and analyzed the data. ZX, TC, RK, HK, KG, ZS and XC wrote and revised the manuscript. TC helped with the mouse experiments. RK and HK provided the *Pax9*$^{loxP/loxP}$ mouse line. KG provided human ESCC tissue sections and clinical data. ZS and XC designed the experiments and supervised the whole process.

References

1. Peters H, Neubuser A, Kratochwil K*, et al.* Pax9-deficient mice lack pharyngeal pouch derivatives and teeth and exhibit craniofacial and limb abnormalities. *Genes Dev* 1998; **12:** 2735–2747.
2. Jonker L, Kist R, Aw A*, et al.* Pax9 is required for filiform papilla development and suppresses skin-specific differentiation of the mammalian tongue epithelium. *Mech Dev* 2004; **121:** 1313–1322.
3. Kist R, Watson M, Crosier M*, et al.* The formation of endoderm-derived taste sensory organs requires a Pax9-dependent expansion of embryonic taste bud progenitor cells. *PLoS Genet* 2014; **10:** e1004709.
4. Nakatomi M, Wang XP, Key D*, et al.* Genetic interactions between Pax9 and Msx1 regulate lip development and several stages of tooth morphogenesis. *Dev Biol* 2010; **340:** 438–449.
5. Sivakamasundari V, Kraus P, Sun W*, et al.* A developmental transcriptomic analysis of Pax1 and Pax9 in embryonic intervertebral disc development. *Biol Open* 2017; **6:** 187–199.
6. Peters H, Schuster G, Neubuser A*, et al.* Isolation of the Pax9 cDNA from adult human esophagus. *Mamm Genome* 1997; **8:** 62–64.
7. Gerber JK, Richter T, Kremmer E*, et al.* Progressive loss of PAX9 expression correlates with increasing malignancy of dysplastic and cancerous epithelium of the human oesophagus. *J Pathol* 2002; **197:** 293–297.
8. Tan B, Wang J, Song Q*, et al.* Prognostic value of PAX9 in patients with esophageal squamous cell carcinoma and its prediction value to radiation sensitivity. *Mol Med Rep*

2017; **16:** 806–816.

9. Lee JC, Sharma M, Lee YH*, et al.* Pax9 mediated cell survival in oral squamous carcinoma cell enhanced by c-myb. *Cell Biochem Funct* 2008; **26:** 892–899.

10. Wang J, Qin R, Ma Y*, et al.* Differential gene expression in normal esophagus and Barrett's esophagus. *J Gastroenterol* 2009; **44:** 897–911.

11. Chen H, Li J, Li H*, et al.* Transcript profiling identifies dynamic gene expression patterns and an important role for Nrf2/Keap1 pathway in the developing mouse esophagus. *PloS One* 2012; **7:** e36504.

12. Chen H, Beasley A, Hu Y*, et al.* A zebrafish model for studies on esophageal epithelial biology. *PloS One* 2015; **10:** e0143878.

13. Sano S, Itami S, Takeda K*, et al.* Keratinocyte-specific ablation of Stat3 exhibits impaired skin remodeling, but does not affect skin morphogenesis. *EMBO J* 1999; **18:** 4657–4668.

14. Kist R, Greally E, Peters H. Derivation of a mouse model for conditional inactivation of Pax9. *Genesis* 2007; **45:** 460–464.

15. Aqeilan RI, Hagan JP, Aqeilan HA*, et al.* Inactivation of the Wwox gene accelerates forestomach tumor progression in vivo. *Cancer Res* 2007; **67:** 5606–5610.

16. Wilkin RJ, Lalor PF, Parker R*, et al.* Murine models of acute alcoholic hepatitis and their relevance to human disease. *Am J Path* 2016; **186:** 748–760.

17. van Dop WA, Rosekrans SL, Uhmann A*, et al.* Hedgehog signalling stimulates precursor cell accumulation and impairs epithelial maturation in the murine oesophagus. *Gut* 2013; **62:** 348–357.

18. Klein ML, Nieminen P, Lammi L*, et al.* Novel mutation of the initiation codon of PAX9 causes oligodontia. *J Dent Res* 2005; **84:** 43–47.

19. Zhou J, Gao Y, Lan Y*, et al.* Pax9 regulates a molecular network involving Bmp4, Fgf10, Shh signaling and the Osr2 transcription factor to control palate morphogenesis. *Development* 2013; **140:** 4709–4718.

20. Kamangar F, Chow WH, Abnet CC*, et al.* Environmental causes of esophageal cancer. *Gastroenterol Clin N Am* 2009; **38:** 27–57, vii.

21. Liu Y, Chen H, Sun Z*, et al.* Molecular mechanisms of ethanol-associated oro-esophageal squamous cell carcinoma. *Cancer Lett* 2015; **361:** 164–173.

22. Ohashi S, Miyamoto S, Kikuchi O*, et al.* Recent advances from basic and clinical studies of esophageal squamous cell carcinoma. *Gastroenterology* 2015; **149:** 1700–1715.

23. Bagnardi V, Blangiardo M, La Vecchia C*, et al.* A meta-analysis of alcohol drinking and cancer risk. *Br J Cancer* 2001; **85:** 1700–1705.

24. Li Y, Mao Y, Zhang Y*, et al.* Alcohol drinking and upper aerodigestive tract cancer mortality: a systematic review and meta-analysis. *Oral Oncol* 2014; **50:** 269–275.

25. Marron M, Boffetta P, Moller H*, et al.* Risk of upper aerodigestive tract cancer and type of alcoholic beverage: a European multicenter case-control study. *Europ J Epidemiol* 2012; **27:** 499–517.

26. Morita M, Kumashiro R, Kubo N*, et al.* Alcohol drinking, cigarette smoking, and the development of squamous cell carcinoma of the esophagus: epidemiology, clinical findings, and prevention. *Intl J Clin Oncol* 2010; **15:** 126–134.

27. Mwachiro MM, Burgert SL, Lando J*, et al.* Esophageal squamous dysplasia is common in asymptomatic Kenyans: a prospective, community-based, cross-sectional study. *Am J Gastroenterol* 2016; **111:** 500–507.

28. Rauch T, Li H, Wu X*, et al.* MIRA-assisted microarray analysis, a new technology for the

determination of DNA methylation patterns, identifies frequent methylation of homeodomain-containing genes in lung cancer cells. *Cancer Res* 2006; **66:** 7939–7947.

29. Tanaka K, Imoto I, Inoue J*, et al.* Frequent methylation-associated silencing of a candidate tumor-suppressor, CRABP1, in esophageal squamous-cell carcinoma. *Oncogene* 2007; **26:** 6456–6468.

30. Khalid O, Kim JJ, Kim HS*, et al.* Gene expression signatures affected by alcohol-induced DNA methylomic deregulation in human embryonic stem cells. *Stem Cell Res* 2014; **12:** 791–806.

31. Berman DM, Karhadkar SS, Maitra A*, et al.* Widespread requirement for Hedgehog ligand stimulation in growth of digestive tract tumours. *Nature* 2003; **425:** 846–851.

32. Santoro A, Pannone G, Papagerakis S*, et al.* Beta-catenin and epithelial tumors: a study based on 374 oropharyngeal cancers. *Biomed Res Int* 2014; **2014:** 948264.

33. Osei-Sarfo K, Tang XH, Urvalek AM*, et al.* The molecular features of tongue epithelium treated with the carcinogen 4-nitroquinoline-1-oxide and alcohol as a model for HNSCC. *Carcinogenesis* 2013; **34:** 2673–2681.

34. Watanabe H, Ma Q, Peng S*, et al.* SOX2 and p63 colocalize at genetic loci in squamous cell carcinomas. *J Clin Invest* 2014; **124:** 1636–1645.

35. Liu K, Jiang M, Lu Y*, et al.* Sox2 cooperates with inflammation-mediated Stat3 activation in the malignant transformation of foregut basal progenitor cells. *Cell Stem Cell* 2013; **12:** 304–315.

36. Lu Y, Futtner C, Rock JR*, et al.* Evidence that SOX2 overexpression is oncogenic in the lung. *PloS One* 2010; **5:** e11022.

Table 1. Incidences of NMBA-induced lesions in mouse esophagus, forestomach, and tongue[a, b]

Group	Genotype	Treatment	No.	Esophagus			Forestomach			Tongue[c]		
				Dysplasia	Papilloma	SCC	Dysplasia	Papilloma	SCC	Dysplasia	Papilloma	SCC
A	Wild-type	Liquid diet	18	0	0	0	22.2% (4/18)	72.2% (13/18)	5.6% (1/18)	0	0	0
B	Wild-type	Isocaloric diet with 6.4% v/v ethanol	24	4.2% (1/24)	50% (12/24) (P=0.0003)	0	16.7% (4/24)	95.8% (23/24)	8.3% (2/24)	0	0	0
C	*Krt5*Cre;*Pax9*$^{loxP/loxP}$	Liquid diet	22	18.2% (4/22)	77.3% (17/22) (P=0.0001)	0	81.8% (18/22) (P=0.0003)	90.9% (20/22)	31.8% (7/22) (P=0.046)	4.5% (1/22)	9.1% (2/22)	22.7% (5/22) (P=0.053)

[a] Microscopically detected lesions including dysplasia, papilloma, and SCC were diagnosed according to established criteria.

[b] All P values were calculated by comparing with Group A and determined using Student's t-test.

[c] P=0.005 when tongue dysplasia, papilloma and SCC are combined for comparison.

Figure Legends

Figure 1. Esophageal phenotypes of *Krt5*Cre;*Pax9*$^{loxP/loxP}$ mice. The papilloma-like structures were formed in the squamous epithelium (indicated by arrows) of *Pax9*-deficient esophagus (B, D) as compared with control esophagus on H&E-stained sections (A, C). Proliferation was increased in *Pax9*-deficient mice (F, H) as compared with controls (E, G). Apoptosis was similar in *Pax9*-deficient esophagus (J) and control esophagus (I), as detected by TUNEL assay. Toluidine blue staining (K, L) and transmission electron microscopy (M, N) showed an increase in keratohyalin granules (red arrows) and disorganization of the basal cell layer in *Pax9*-deficient esophagus as compared with control esophagus. Double IF showed that Ki67 was exclusively expressed in the basal cells of esophageal epithelium in control esophagus (O, Q, S, U) at the fifth day after BrdU pulse injection. However, in the mutant esophagus, some Ki67 positive cells appeared in the parabasal and superficial layers, and they were also BrdU-positive with the same staining intensity as the BrdU-positive cells in the basal cell layer (P, R, T, V) (yellow arrows). The base membrane of the squamous epithelium was marked with white dotted lines. (A, B, E, F, I, J: Scale bar=200 μm. C, D, G, H, O, P, Q, R, S, T, U, V: Scale bar=50 μm. K, L: Scale bar=20 μm. M, N: Scale bar=2 μm).

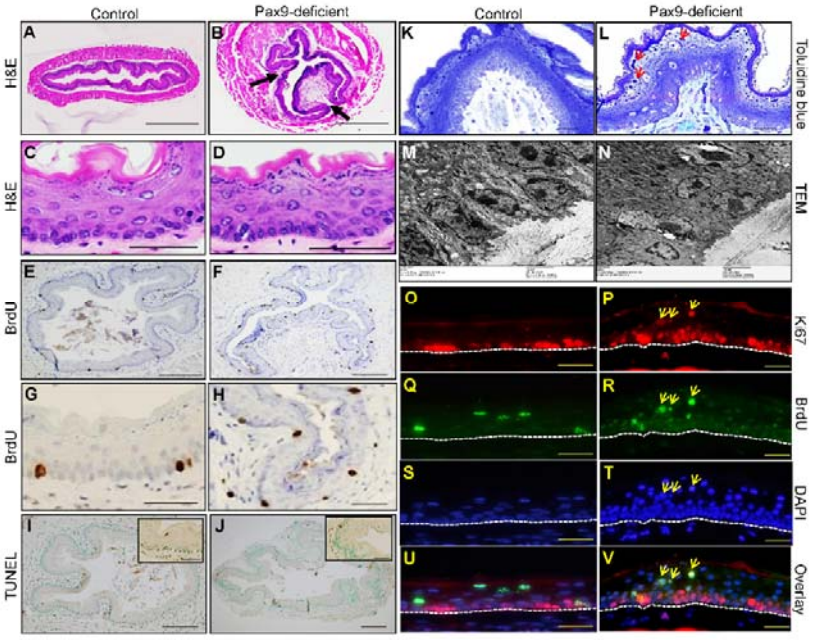

Figure 2. Differentially expressed genes in *Krt5*Cre;*Pax9*$^{loxP/loxP}$ esophagus. Control and mutant esophagus were clustered based on differential expression of genes identified by SAM (A). IHC showed expression of SOX2 (B, C: Scale bar=50 μm), FOXA3 (D, E: Scale bar=50 μm), WNT3 (F, G: Scale bar=50 μm), SFRP5 (H, I: Scale bar=100 μm), KRT35 (J, K: Scale bar=50 μm), KRT5 (L, M: Scale bar=50 μm), P63 (N, O: Scale bar=50 μm), filaggrin (P, Q: Scale bar=50 μm), involucrin (R, S: Scale bar=50 μm) and loricrin (T, U: Scale bar=50 μm) in the mutant esophagus as compared with the wild-type esophagus. Bar represents mean ± SD.

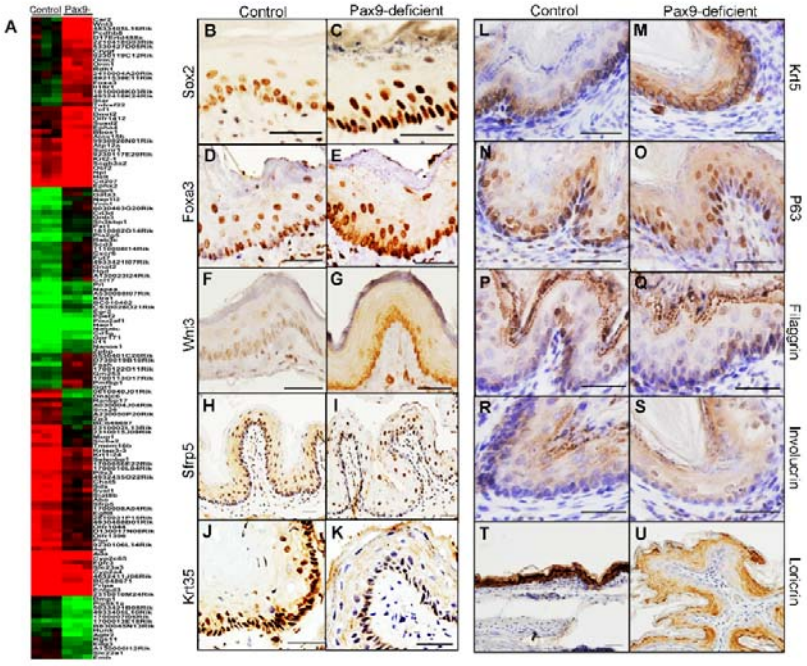

Figure 3. Down-regulation of PAX9 expression in human ESCC and OSCC. Paraffin sections of human ESCC were confirmed for histopathology by H&E staining (A, B) and stained for PAX9 (C, D). The percentage of PAX9-positive cells was determined as the number of PAX9-positive cells divided by the number of epithelial cells (E). Based on the drinking status of these patients (drinker or non-drinker), PAX9 expression was compared between drinker's normal tissue and non-drinker's normal tissue, and between drinker's cancer tissue and non-drinker's cancer tissue (F). Bar represents mean ± SD. Scale bar=100 μm. P values were determined using Student's t-test.

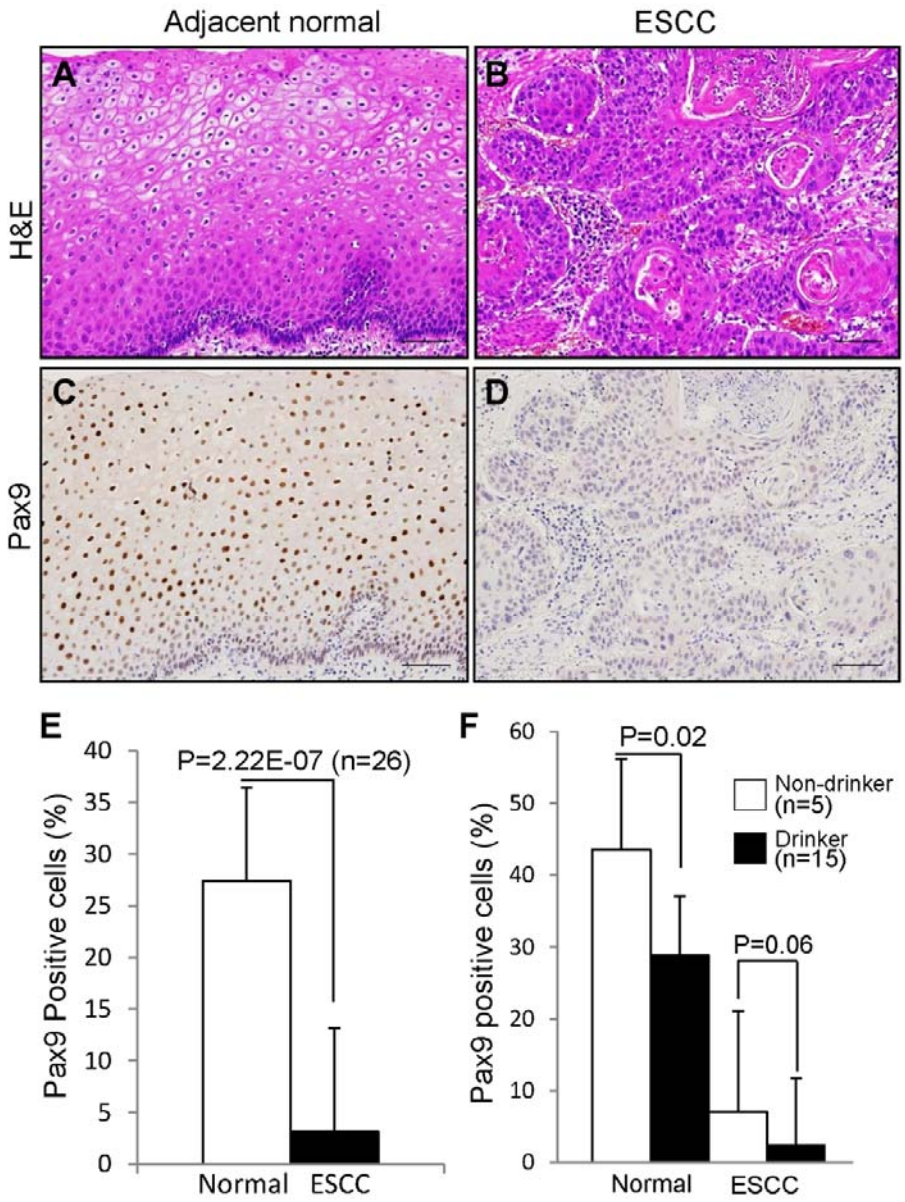

Figure 4. Down-regulation of PAX9 expression in squamous epithelial cells of mouse forestomach due to alcohol drinking *in vivo*. Ethanol caused thickening and basal cell hyperproliferation in mouse forestomach (A, B, C; H&E staining). Epithelial hyperproliferation in mouse forestomach was validated by BrdU IHC (D, E, F) and quantitation (G). Hierarchical clustering analysis of gene microarray data

showed that *Pax9* gene set was enriched in the non-exposed mouse forestomach as compared with those exposed to ethanol (H). Loricrin IHC showed that ethanol inhibited differentiation of the squamous epithelial cells in mouse forestomach (I, J, K). PAX9 IHC (L, M, N), PAX9 Western blotting (O, P), and RT-qPCR (Q) confirmed down-regulation of *Pax9* mRNA and protein in the squamous epithelial cells in mouse forestomach. Broken lines are placed to indicate alignment of the group lanes. * P <.05, ** P <.01. Bar represents mean ± SD. Scale bar=50 μm. P values were determined using Student's t-test.

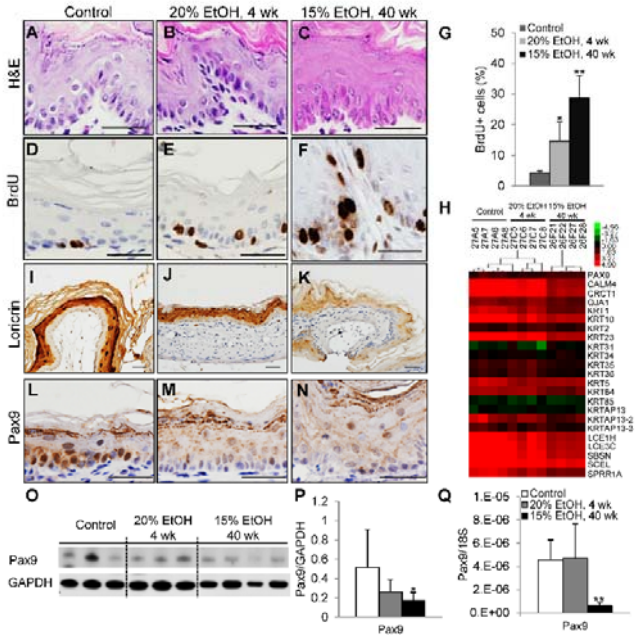

Figure 5. PAX9 promoter hypermethylation in KYSE70 cells and human OSCC samples. KYSE70 cells treated with different concentrations of DAC were analyzed by Western blotting for PAX9 expression (A). The percentages of methylation at CpG sites in the promoter regions of two different *PAX9* transcriptional start sites were analyzed by pyrosequencing for comparison between control and DAC-treated KYSE70 cells (B, n=3; * P <.05). The percentage of methylation at CpG sites in the promoter regions of two different *PAX9* transcriptional start sites were analyzed by pyrosequencing for comparison between human OSCC and matched normal samples (C, n=6; * P <.05). P values were determined using Student's t-test.

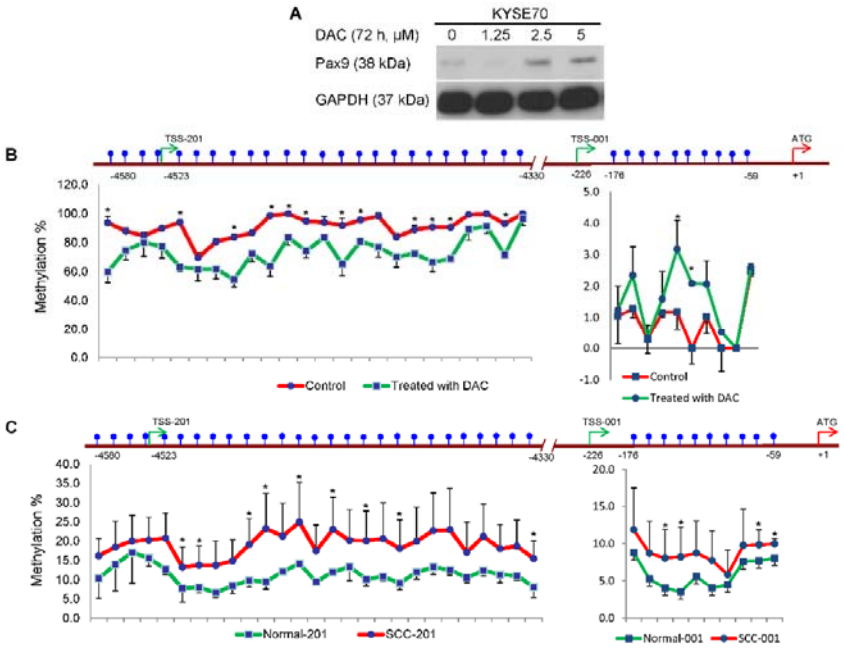

Figure 6. Promotion of NMBA-induced tumorigenesis in mouse forestomach due to *Pax9* deficiency or alcohol drinking. The number of macroscopically visible tumors in mouse forestomach increased significantly in mice fed with an isocaloric *Lieber-DeCarli* diet containing ethanol (Group B) and *Pax9*-deficient mice (Group C), as compared with control (Group A) (A, * P <.05, *** P <.001). The middle red lines show the averages. Esophageal dysplasia (B), papilloma (C), SCC (D), forestomach dysplasia (E), papilloma (F), SCC (G), and tongue dysplasia (H), SCC (I) are shown here (B, E, H, Scale bar=50 μm; C, D, F, G, I, Scale bar=100 μm). P values were determined using Student's t-test.

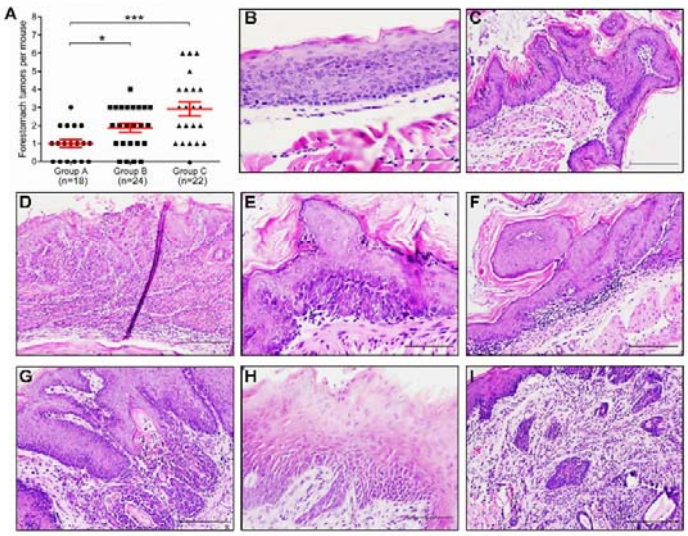

SUPPLEMENTARY MATERIAL ONLINE

Supplementary figure legends

Figure S1. Generation and validation of *Krt5*Cre;*Pax9*$^{loxP/loxP}$ mice

Figure S2. Differentially expressed genes in *Krt5*Cre;*Pax9*$^{loxP/loxP}$ esophagus

Figure S3. *Pax9* down-regulation in human ESCC (A, B) and OSCC (C, D) in comparison with matched normal tissues

Figure S4. Down-regulation of PAX9 expression in esophageal squamous epithelial cells exposed to ethanol *in vitro*

Figure S5. Differentially expressed genes and gene sets in mouse forestomach due to alcohol drinking

Figure S6. Down-regulation of PAX9 expression in mouse tongue due to alcohol drinking

Figure S7. Human *PAX9* and mouse *Pax9* gene promoter regions for pyrosequencing

Figure S8. Pyrosequencing of the *PAX9* promoter after ethanol exposure (KYSE510 cells) or alcohol drinking (mouse forestomach)

Figure S9. Pax9 expression in histologically normal epithelium (A), NMBA-exposed histologically normal epithelium (B), NMBA-induced dysplasia (C) and NMBA-induced forestomach SCC (D)

Table S1. Differentially expressed genes and enriched gene sets in *Pax9*-deficient esophagus as compared with control esophagus

Table S2. Differentially expressed genes and enriched gene sets in mouse forestomach due to alcohol drinking (20% in the drink for 4 weeks or 15% in the drink for 40 weeks)